

# Sharing Resources Can Lead to Monostability in a Network of Bistable Toggle Switches\*

Andras Gyorgy<sup>1</sup>

**Abstract**—The vision of synthetic biology is to engineer complex cellular systems in a modular fashion. Unfortunately, multiple factors hinder such modular design, thus the scalability of rationally engineering synthetic gene circuits. One major barrier emerges due to the limited availability of shared cellular resources, intertwining the behavior of otherwise disconnected components. It was recently demonstrated that these unwanted and pervasive coupling effects can be accurately predicted both *in vitro* and *in vivo*. Here, we not only analyze how these effects influence the collective behavior of multiple toggle switches, but we also illustrate how to leverage this predominantly disadvantageous coupling. In particular, we prove that by turning on/off a load module, the network of toggle switches can be switched between monostable and multistable modes. Importantly, this can be achieved without any direct regulatory connection among the toggle switches or between the load module and any of the toggle switches, thus presenting a major experimental advantage over relying on traditional regulatory linkages. This idea of exploiting and leveraging resource competition is illustrated through the design of a cellular random number generator.

## I. INTRODUCTION

While the fundamental goal of synthetic biology is to design and implement complex behaviors at both the cellular and the population levels, our current ability to create such systems is severely limited. Instead of rationally engineering large-scale synthetic gene circuits, today numerous iterative cycles of designing, building and testing parts are required for creating systems of modest complexity. This approach most often relies on the creation of large libraries containing a vast number of slightly different designs [1], [2]. Instead of such costly and slow trial-and-error experimental approaches, computational tools enable the rational design of complex synthetic gene circuits in a predictable fashion, thus directly addressing their scalability issue by significantly decreasing both cost and time of development [3], [4].

Accordingly, the broad topic of context-dependence has lately become a central theme in synthetic biology [5], [6], [7], [8], [9]. One fundamental source of context-dependence is the limited availability of shared cellular resources [9], [10], [11], [12], [13], causing unwanted coupling among otherwise disconnected modules. We have recently developed a mathematical model capturing the effects of competition for shared resources, with model predictions matching experimental data both *in vitro* and *in vivo* [12], [13]. As a result, unwanted coupling effects can be accounted for during systems-level design, demonstrated in this paper.

\*This work was not supported by any organization

<sup>1</sup>Andras Gyorgy is with the Department of Electrical and Computer Engineering, New York University Abu Dhabi, UAE andras.gyorgy@nyu.edu

Despite their simplicity, toggle switches provide the basis of a variety of modules, such as clocks [14] and frequency multipliers [15]. As a result of their widespread use, it is thus imperative to understand how the fundamental phenomenon of resource competition shapes the behavior of this basic building block of synthetic biology, setting the stage for the results of this paper. We first prove that if resource sequestration exceeds a critical threshold, a bistable toggle switch suddenly becomes monostable. Following this, we next prove that the collective behavior of a network of bistable toggle switches can become monostable due to the limited availability of shared resources. Therefore, scarcity of common resources acts against both bistability and multistability. Importantly, coupling among components is realized indirectly, through the common pool of shared resources. As a result, turning on/off a separate load module can trigger monostable/multistable transitions in a network of otherwise disconnected toggle switches. Illustrating this, we design a random number generator by leveraging resource competition and cellular noise, both inherent to living systems.

Our results provide explicit guidelines for the design of large-scale systems by characterizing the effects of shared resources. In addition to this, we demonstrate that these effects are not necessarily adverse: instead of minimizing/eliminating them, they can be leveraged and incorporated directly into the design of complex systems as we illustrate here. This innovative approach together with the availability of orthogonal resources [16] thus paves the path for novel ways to control and interact with cellular systems.

This paper is organized as follows. After reviewing the mathematical model of the toggle switch with scarce resources, we next derive the stability results for both a single toggle switch and also for a network interconnection of them. Finally, we demonstrate how to leverage resource competition by designing a cellular random number generator.

## II. MATHEMATICAL MODEL AND PROBLEM FORMULATION

The toggle switch was one of the first synthetic gene circuits, comprising two proteins ( $y$  and  $z$ ) repressing each other's expression [17], given by the dimensionless model

$$\dot{y} = \alpha_y \frac{1}{1 + z^n} - y, \quad \dot{z} = \alpha_z \frac{1}{1 + y^n} - z. \quad (1)$$

In case of a symmetric switch (i.e.,  $\alpha_y = \alpha_z =: \alpha > 0$ ), a simple condition has been derived in [17] ensuring bistability.

**Theorem 1** ([17]). *The system in (1) is monostable if  $n = 1$ . If  $n = 2$ , it is bistable if  $\alpha > 2$  and monostable otherwise.*

The above model, however, neglects the fact that many resources (RNA polymerase, ribosomes, etc.) are shared for the production of  $y$  and  $z$ , and these resources are only available in limited quantities [10], [11], [12], [13]. In particular, when accounting for the limited availability of shared transcriptional/translational resources, according to [12], [13] the de-dimensionalized dynamics of the toggle switch with repressor proteins  $y$  and  $z$  become

$$\begin{aligned}\dot{y} &= \frac{\alpha_y \frac{1}{1+z^n}}{1 + \beta_y \frac{1}{1+z^n} + \beta_z \frac{1}{1+y^n}} - y, \\ \dot{z} &= \frac{\alpha_z \frac{1}{1+y^n}}{1 + \beta_y \frac{1}{1+z^n} + \beta_z \frac{1}{1+y^n}} - z,\end{aligned}\quad (2)$$

where the lumped constants  $\alpha_w$  and  $\beta_w$  for  $w \in \{y, z\}$  depend on measurable and tunable biophysical parameters (see the Supplementary Material for more details and typical values). Comparing (1) with (2) we can interpret  $\beta_y$  and  $\beta_z$  quantifying how the production of  $y$  and  $z$ , respectively, exerts a load on the common pool of shared resources. Therefore, in what follows we focus on these parameters, and assume that  $\alpha_y = \alpha_z =: \alpha$  to simplify our analysis.

In the case of multiple toggle switches all competing for the same resources, from [12], [13] their dynamics become

$$\begin{aligned}\dot{y}_i &= \frac{\alpha \frac{1}{1+z_i^n}}{1 + \sum_{i=1}^N \left( \frac{\beta_{y,i}}{1+z_i^n} + \frac{\beta_{z,i}}{1+y_i^n} \right) + \beta_L(t)} - y_i, \\ \dot{z}_i &= \frac{\alpha \frac{1}{1+y_i^n}}{1 + \sum_{i=1}^N \left( \frac{\beta_{y,i}}{1+z_i^n} + \frac{\beta_{z,i}}{1+y_i^n} \right) + \beta_L(t)} - z_i\end{aligned}\quad (3)$$

for  $i = 1, 2, \dots, N$ , where  $\beta_{y,i}$  and  $\beta_{z,i}$  characterize the resource usage of the production of  $y_i$  and  $z_i$ , respectively, and similarly,  $\beta_L(t)$  captures the resource sequestration of modules other than the toggle switches (regarded as load). From (3) it follows that the behaviors of the toggle switches are now intertwined via the limited availability of the shared resources through the constants  $\beta_{y,i}$  and  $\beta_{z,i}$ .

In this paper, we seek to answer the following questions. How does resource competition alter the results of Thm. 1? Does loading within a single toggle switch promote or hinder bistability? How does loading external to a single toggle switch affect its stability profile? What kinds of behaviors emerge when multiple bistable toggle switches compete for the same resources? After answering these questions, we will illustrate that competition for shared resources can be leveraged in a novel way to control multiple modules simultaneously without any direct regulatory linkages.

### III. RESULTS

After characterizing how resource competition shapes the stability profile of a single toggle switch ( $N = 1$ ), we will extend these results to the case of multiple modules ( $N = 2, 3, \dots$ ) when  $\beta_L(t) \equiv \beta_L \geq 0$ , i.e., resource sequestration of components other than the toggles is constant. Leveraging time-varying  $\beta_L(t)$  is the focus of the next section.

#### A. Bistability of a Single Toggle Switch

Since we consider first the case of a single toggle switch ( $N = 1$ ), we drop the subscript  $i$  in (3), thus yielding with  $u := \beta_y/(1+z^n) + \beta_z/(1+y^n)$  the dynamics

$$\dot{y} = \frac{\alpha \frac{1}{1+z^n}}{1+u+\beta_L} - y, \quad \dot{z} = \frac{\alpha \frac{1}{1+y^n}}{1+u+\beta_L} - z. \quad (4)$$

**Proposition 1.** *The system in (4) is monostable if  $n = 1$ .*

*Proof.* With  $\rho := 2(1+\beta_L)/(1+\beta_y+\beta_z+\beta_L)$  we obtain  $y = z = (-1 + \sqrt{1 + \alpha\rho^2/(1+\beta_L)})/\rho$  at the unique positive equilibrium. Stability follows from nullcline analysis.  $\square$

Therefore, the limited availability of shared resources does not change the fact that multimerization is necessary for obtaining bistability (Thm. 1, adopted from [17]), so that for the remainder of the paper we consider dimerization ( $n = 2$ ).

**Definition 1.** The equilibrium  $x \in \mathbb{R}^m$  of the dynamical system  $\dot{x} = f(x)$  is called *specular* if  $x_1 = \dots = x_m$ .

**Definition 2.** The equilibrium  $x \in \mathbb{R}^m$  of the dynamical system  $\dot{x} = f(x)$  is called *hyperbolic* if the Jacobian  $\partial f/\partial x$  has no eigenvalues with zero real parts at this equilibrium.

**Theorem 2.** *Define  $\bar{\beta}_w := 1 + \beta_w + \beta_L$  for  $w \in \{y, z\}$  and let  $\bar{\beta} := \sqrt{\bar{\beta}_y \bar{\beta}_z}$ . The system in (4) is bistable if  $\alpha > 2\bar{\beta}$ , and the two stable non-specular hyperbolic equilibria are given by  $(y, z) = (y^+, z^-)$  and  $(y, z) = (y^-, z^+)$  with*

$$w^{+,-} := \frac{\alpha}{2\bar{\beta}_w} \left( 1 \pm \sqrt{1 - \left( \frac{2\bar{\beta}}{\alpha} \right)^2} \right), \quad w \in \{y, z\}. \quad (5)$$

*If  $2\bar{\beta} > \alpha$  then (4) is monostable such that  $0 < y = z < 1$  at the unique stable specular hyperbolic equilibrium.*

*Proof.* Rewrite (4) as  $\dot{y} = f_y(y, z)$  and  $\dot{z} = f_z(y, z)$ . Setting  $f_y(y, z) = f_z(y, z) = 0$  yields  $y/(1+y^2) = z/(1+z^2)$ , thus either  $y = z$  or  $y = 1/z$  at the equilibrium of (4).

When  $y = z$ , from  $f_w(w, w) = 0$  for  $w \in \{y, z\}$  we obtain that  $0 = (1 + \beta_L)w^3 + (1 + \beta_y + \beta_z + \beta_L)w - \alpha =: h(w)$ , yielding the discriminant  $\Delta = -27\alpha^2(1 + \beta_L)^2 - 4(1 + \beta_L)(1 + \beta_y + \beta_z + \beta_L)^3 < 0$ . Thus,  $h(w) = 0$  has one real root and two non-real complex conjugate roots. Since the number of sign differences between consecutive nonzero coefficients of  $h(w)$  is precisely one, we conclude that the unique real root  $w$  of  $h(w) = 0$  is positive by Descartes' rule of signs, yielding a specular equilibrium of (4).

When  $y = 1/z$ , from  $f_y(y, 1/y) = f_z(1/z, z) = 0$  we obtain that  $yg_y(y) = zg_z(z) = 0$  with  $g_y := \bar{\beta}_y y^2 - \alpha y + \bar{\beta}_z$  and  $g_z(z) := \bar{\beta}_z z^2 - \alpha z + \bar{\beta}_y$ . Since  $y = 0$  would yield  $z \rightarrow \infty$  in this case, we must have  $g_y(y) = g_z(z) = 0$  at an equilibrium of (4). The discriminant of both  $g_y(y) = 0$  and  $g_z(z) = 0$  is given by  $\alpha^2 - 4\bar{\beta}^2$ , hence the roots are non-real complex conjugates if  $2\bar{\beta} > \alpha$ , whereas if  $2\bar{\beta} < \alpha$  then both roots are positive (as the coefficient of the first order term is negative), and are given by  $w^{+,-}$  for  $w \in \{y, z\}$  in (11), respectively. In this latter case, of the four possible combinations (two roots for each quadratic polynomial) only

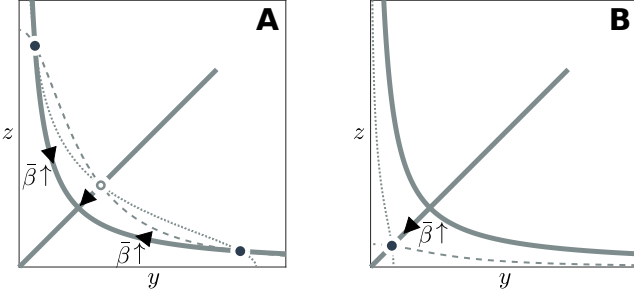


Fig. 1. Competition for shared resources acts against bistability. Nullclines of (4) are depicted with thin lines (dotted for  $f_y(y, z) = 0$  and dashed for  $f_z(y, z) = 0$ ), solid thick lines correspond to  $y = z$  and  $y = 1/z$ . (A) The toggle switch in (4) is bistable as long as  $\alpha > 2\bar{\beta} \geq 2$ . As  $\bar{\beta}$  increases, the two stable non-specular equilibria (black full circles) slide along  $z = 1/y$  towards each other, while the unique unstable specular equilibrium (gray empty circle) slides along  $z = y$  towards the origin. (B) Once  $2\bar{\beta} > \alpha$ , the toggle switch in (4) becomes monostable such that the unique stable specular equilibrium continues to slide along  $y = z$  towards the origin.

$(y, z) = (y^+, z^-)$  and  $(y, z) = (y^-, z^+)$  yield  $yz = 1$ , thus only these two are (non-specular) equilibria of (4).

To conclude the stability of the above three equilibria, consider the nullclines  $0 = f_y(y, z)$  and  $0 = f_z(y, z)$  in Fig. 1 (dotted and dashed lines, respectively). First, from (4) it follows that  $\frac{\partial f_y}{\partial z}, \frac{\partial f_z}{\partial y} < 0$ . Second, at the equilibria denoted by black circles, we have

$$\left. \frac{dz}{dy} \right|_{f_y(y,z)=0} < \left. \frac{dz}{dy} \right|_{f_z(y,z)=0} < 0,$$

so that we obtain  $\frac{\partial f_y}{\partial y}, \frac{\partial f_z}{\partial z} < 0$ , hence  $\frac{\partial f_y}{\partial y} + \frac{\partial f_z}{\partial z} < 0$ , together with  $\frac{\partial f_y}{\partial y} \frac{\partial f_z}{\partial z} - \frac{\partial f_y}{\partial z} \frac{\partial f_z}{\partial y} > 0$ . Thus, the trace and determinant of the Jacobian of (4) are negative and positive, respectively, about the equilibria denoted by black circles in Fig. 1. Hence, these equilibria are stable and hyperbolic. Instability of the equilibrium denoted by the empty circle can be shown similarly.

All there is left to show is that  $0 < y = z < 1$  at the unique stable specular equilibrium in Fig. 1B. To this end, note that  $y = z$  is invariant for (4), and since  $f_y(0, 0), f_z(0, 0) > 0$  and  $f_y(1, 1), f_z(1, 1) < 0$  if  $2\bar{\beta} > \alpha$ , there is an equilibrium on the segment connecting the origin with  $(1, 1)$ . Since there is only one equilibrium in this case, we have  $0 < y = z < 1$  at the unique stable and hyperbolic equilibrium.  $\square$

Resource competition thus acts against bistability (Fig. 1) by increasing the critical threshold for  $\alpha$  from 2 to  $2\bar{\beta} \geq 2$ . The effects of loading within the toggle switch ( $\beta_y$  and  $\beta_z$ ) and originating outside of it ( $\beta_L$ ) are combined in the lumped parameter  $\bar{\beta} > 1$ .

### B. Multistability of a Network of Toggle Switches

Although different toggle switches do not directly affect each other, their dynamics are coupled according to (3) due to competition for shared resources. Here we focus on how this coupling shapes the collective behavior of the network when  $n = 2$ . For simpler notation, we assume that individual toggles are symmetric ( $\beta_{y,i} = \beta_{z,i} =: \beta_i$ ), but allow for a

set of different toggle switches ( $\beta_i$  and  $\beta_j$  can be different). Rewrite the dynamics in (3) for  $i = 1, 2, \dots, N$  as

$$\begin{aligned} \dot{y}_i &= \frac{\alpha \frac{1}{1+z_i^2}}{1 + \frac{\beta_i}{1+z_i^2} + \frac{\beta_i}{1+y_i^2} + v_i + \beta_L} - y_i, \\ \dot{z}_i &= \frac{\alpha \frac{1}{1+y_i^2}}{1 + \frac{\beta_i}{1+z_i^2} + \frac{\beta_i}{1+y_i^2} + v_i + \beta_L} - z_i \end{aligned} \quad (6)$$

with  $v_i := \sum_{j \neq i} \beta_j \left( \frac{1}{1+z_j^2} + \frac{1}{1+y_j^2} \right)$ .

While the single toggle switch in (4) is monotone with respect to the positive orthant, the networked system in (3) is not monotone with respect to any orthant [18], [19]. Additionally, we are unable to conclude monotonicity of (3) with respect to more general positivity cones using the results in [19] either as the modules in (6) have no non-degenerate input to state (I/S) static characteristic (since it is not true that for each constant input there exists a unique globally asymptotically stable equilibrium due to the bistability discussed in Thm. 2). To overcome this limitation, we will analyze the stability of the equilibria of (6) based on stability properties of a planar auxiliary dynamical system.

**Lemma 1.** Introduce  $x := (y, z)^\top$ , together with

$$g(w, u) := \frac{\alpha \frac{1}{1+w^2}}{1 + u + \beta_L}, \quad h(x) := \frac{1}{1+y^2} + \frac{1}{1+z^2}, \quad (7)$$

$$\lambda := \sum_{i=1}^N \beta_i, \quad f(x, u) := \begin{pmatrix} g(z, u) - y \\ g(y, u) - z \end{pmatrix}. \quad (8)$$

If  $x_0$  is an asymptotically stable hyperbolic equilibrium of both  $\dot{x} = f(x, \lambda h(x_0))$  and  $\dot{x} = f(x, \lambda h(x))$ , then so is  $x_i := (y_i, z_i)^\top = x_0$  for  $i = 1, 2, \dots, N$  of (6).

*Proof.* Let  $\mathbf{1}_N \in \mathbb{R}^N$  and  $I_N \in \mathbb{R}^{N \times N}$  denote the column vector with entries 1 and the identity matrix, respectively.

Rewrite (6) with  $u_i := \sum_{i=1}^N \beta_i h(x_i)$  as

$$\dot{x}_i = f(x_i, u_i) \quad i = 1, 2, \dots, N. \quad (9)$$

Therefore, if  $f(x_0, \lambda h(x_0)) = 0$  then  $\mathbf{1}_N \otimes x_0$  is an equilibrium of (9). Thus, all there is left to show is that the Jacobian of (9) about  $\mathbf{1}_N \otimes x_0$  is Hurwitz.

To prove this, define  $P := \mathbf{1}_N \otimes (\beta_1 \dots \beta_N) \in \mathbb{R}^{N \times N}$  together with  $A := \partial f(x, u) / \partial x$ ,  $B := \partial f(x, u) / \partial u$ , and  $C := dh(x) / dx$ , all evaluated at  $(x, u) = (x_0, \lambda h(x_0))$ . With this, the Jacobian of (9), thus of (6) about the equilibrium  $\mathbf{1}_N \otimes x_0$  is  $I_N \otimes A + P \otimes (BC)$ . Its eigenvalues are those of  $A + \lambda_k BC$  where  $\lambda_k$  is the eigenvalue of  $P$  for  $k = 1, 2, \dots, N$  (see Lem. S1 in the Supplementary Material of [20]).

Since  $\text{rank}(P) = 1$ , it has a single non-zero eigenvalue, given by  $\lambda$ . As the Jacobians of both  $\dot{x} = f(x, \lambda h(x_0))$  and  $\dot{x} = f(x, \lambda h(x))$  about  $x_0$  are  $A$  and  $A + \lambda BC$ , respectively, they are both Hurwitz by supposition. Therefore, so is the matrix  $I_N \otimes A + P \otimes (BC)$ , thus  $\mathbf{1}_N \otimes x_0$  is an asymptotically stable hyperbolic equilibrium of (6).  $\square$

**Theorem 3.** *The system in (6) is multistable if*

$$2\beta < \alpha - 2 \max_i \sum_{j \neq i} \beta_j \quad (10)$$

with  $\beta := 1 + \beta_L + \sum_{i=1}^N \beta_i$ . In particular, in this case there are  $2^N$  asymptotically stable hyperbolic equilibria such that either  $(y_i, z_i) = (w^+, w^-)$  or  $(y_i, z_i) = (w^-, w^+)$  with

$$w^{+,-} := \frac{\alpha}{2\beta} \left( 1 \pm \sqrt{1 - \left( \frac{2\beta}{\alpha} \right)^2} \right). \quad (11)$$

Conversely, (6) is monostable if

$$2\beta > \alpha \quad (12)$$

such that  $0 < y_1 = \dots = y_N = z_1 = \dots = z_N < 1$  at the unique stable hyperbolic equilibrium.

*Proof.* The proof comprises three main parts (additional details are provided in the Supplementary Material). We first localize the fixed points and rule out the clearly unstable ones. Second, we prove that the remaining  $2^N$  non-specular fixed points are asymptotically stable and hyperbolic. Third, we repeat this for the unique specular equilibrium.

We will leverage Thm. 2 to study the fixed points of (6). To this end, let  $x_i := (y_i \ z_i)^\top$  and with  $h(\cdot)$  from (7) introduce  $b_i := \beta_L + \sum_{j \neq i} \beta_j h(x_j)$ , so that (6) becomes

$$\begin{aligned} \dot{y}_i &= \frac{\alpha \frac{1}{1+z_i^2}}{1 + \beta_i h(x_i) + b_i} - y_i, \\ \dot{z}_i &= \frac{\alpha \frac{1}{1+y_i^2}}{1 + \beta_i h(x_i) + b_i} - z_i. \end{aligned} \quad (13)$$

Furthermore, let  $b_i^0$  denote the value of  $b_i$  at a given stable equilibrium, which will play the role of  $\beta_L$  in Thm. 2.

*a) Location of potentially stable fixed points:* Consider first the case when  $2(1 + \beta_i + b_i^0) < \alpha$ , so that it follows from Thm. 2 that the nullclines of (13) in the  $(y_i, z_i)$ -plane have three intersections (Fig. 1A): an unstable specular solution and two potentially stable non-specular solutions such that  $y_i z_i = 1$ . Therefore, if  $2(1 + \beta_i + b_i^0) < \alpha$  holds for  $i = 1, 2, \dots, N$ , then the potentially stable solutions are all non-specular such that  $y_i z_i = 1$  for all  $i = 1, 2, \dots, N$ , thus  $h(x_i) = 1$ , and as a result,  $b_i^0 = \beta_L + \sum_{j \neq i} \beta_j$ . Thus, at the potentially stable (non-specular) solutions we obtain from Thm. 2 that either  $(y_i, z_i) = (w^+, w^-)$  or  $(y_i, z_i) = (w^-, w^+)$  with  $w^{+,-}$  from (11). In part b) of this proof we show that all  $2^N$  such non-specular equilibria are asymptotically stable and hyperbolic.

Second, if  $2(1 + \beta_i + b_i^0) > \alpha$  then it follows from Thm. 2 that the nullclines of (13) in the  $(y_i, z_i)$ -plane have a unique intersection (Fig. 1B), corresponding to a potentially stable specular solution such that  $0 < y_i = z_i < 1$ . Therefore, if  $2(1 + \beta_i + b_i^0) > \alpha$  holds for  $i = 1, 2, \dots, N$ , then there is a unique potentially stable (specular) solution such that  $0 < y_i = z_i < 1$  for  $i = 1, 2, \dots, N$ , thus  $1 < h(x_i) < 2$ , and as a result,  $b_i^0 < \beta_L + 2 \sum_{j \neq i} \beta_j$ . Furthermore, since in this case (13) are identical for  $i = 1, 2, \dots, N$  at this

unique equilibrium, so are their unique solutions  $y_i$  and  $z_i$ , thus  $0 < y_1 = \dots = y_N = z_1 = \dots = z_N < 1$  (see the Supplementary Material for additional details). In part c) of this proof we show that this unique specular equilibrium is asymptotically stable and hyperbolic.

Finally, we have already seen above that at a stable equilibrium we have  $\beta_L + \sum_{j \neq i} \beta_j \leq b_i^0 < \beta_L + 2 \sum_{j \neq i} \beta_j$ . It follows directly from this that (10) and (12) yield the conditions  $2(1 + \beta_i + b_i^0) < \alpha$  and  $2(1 + \beta_i + b_i^0) > \alpha$ , respectively, for  $i = 1, 2, \dots, N$  (see the Supplementary Material for additional details).

*b) Stability of the non-specular fixed points:* Here, we prove that the  $2^N$  potentially stable non-specular equilibria identified in part a) of this proof are all asymptotically stable and hyperbolic. We prove stability of non-specular equilibria of the form  $\mathbf{1}_N \otimes x_0$  with  $x_0 := (w^+, w^-)^\top$ , stability of other non-specular equilibria obtained by  $w^+ \leftrightarrow w^-$  swappings for  $y_i \leftrightarrow z_i$  follows due to  $y_i \leftrightarrow z_i$  symmetry of (13).

In part a) of this proof we showed that (10) yields  $2^N$  potentially stable non-specular equilibria such that  $y_i z_i = w^+ w^- = 1$ . As a result, we have  $h(x_0) = 1$ , thus with  $\lambda$  from (8) we obtain that

$$2(1 + \beta_L + \lambda) < \alpha. \quad (14)$$

First, from (14) we obtain that  $\alpha/[1 + \lambda h(x_0) + \beta_L] > 2$ , thus from Thm. 1 it follows that  $\dot{x} = f(x, \lambda h(x_0))$  is bistable, hence its non-specular equilibrium  $x_0$  is hyperbolic and asymptotically stable (to see that it is hyperbolic, invoke Thm. 2 with  $\beta_y = \beta_z = \beta_L = 0$ ).

Second, referring to Thm. 2 with  $\beta_y := \lambda$  and  $\beta_z := \lambda$ , we have that  $\bar{\beta} = 1 + \lambda + \beta_L$ , so that (14) is equivalent to  $\alpha > 2\bar{\beta}$ . Therefore, from Thm. 2 it follows that  $\dot{x} = f(x, \lambda h(x))$  is bistable, thus its non-specular equilibrium  $x_0$  is hyperbolic and asymptotically stable.

Taken together, the above two results yield from Lem. 1 that the non-specular equilibrium  $\mathbf{1}_N \otimes x_0$  of (6) is hyperbolic and asymptotically stable in case of (10).

*c) Stability of the unique specular fixed point:* Here, we prove that the unique potentially stable specular equilibrium  $0 < y_1 = \dots = y_N = z_1 = \dots = z_N < 1$  identified in part a) of this proof is asymptotically stable and hyperbolic. From (12) with  $\lambda$  defined in (8) it follows that

$$2(1 + \beta_L + \lambda) > \alpha, \quad (15)$$

and since  $0 < y_i = z_i < 1$  we now have  $1 < h(x_0) < 2$  at the equilibrium with  $x_0 := (y_i, z_i)^\top$ . Thus, from (15) we obtain that  $\alpha/[1 + \beta_L + \lambda h(x_0)] < 2$ . The proof concludes by invoking Thm. 1–2 and Lem. 1 as in part b), see the Supplementary Material for additional details.  $\square$

Therefore, the emergent collective behavior of a network of toggle switches is multistable only if the overall loading is sufficiently small, captured by (10). Conversely, a collection of individually bistable toggle switches becomes monostable due to competition for shared resources if

$$1 + \beta_L + \max_i \beta_i < \frac{\alpha}{2} < 1 + \beta_L + \sum_{i=1}^N \beta_i.$$

## IV. APPLICATION EXAMPLE

Next, we focus on the case when loading from the context of the network of toggle switches is modulated (Fig. 2A) between  $\beta_L^{\text{MULTI}}$  and  $\beta_L^{\text{MONO}}$  such that with  $\lambda$  from (8)

$$\beta_L^{\text{MULTI}} < \frac{\alpha}{2} - (1 + \lambda + \max_i \sum_{j \neq i} \beta_j), \quad \beta_L^{\text{MONO}} > \frac{\alpha}{2} - (1 + \lambda).$$

While in the former case the network is multistable, in the latter it becomes monostable (Thm. 3), thus the profiles in the  $(y_i, z_i)$ -planes alternate between those in Fig. 1.

Following a  $\beta_L^{\text{MULTI}} \rightarrow \beta_L^{\text{MONO}}$  switch the unique stable equilibrium is such that  $0 < y_1 = z_1 = \dots = y_N = z_N < 1$  (phase ① in Fig. 2B). Conversely, after a  $\beta_L^{\text{MONO}} \rightarrow \beta_L^{\text{MULTI}}$  switch the system trajectory evolves along the separatrix in Fig. 1A in all  $(y_i, z_i)$ -planes, approaching the unstable equilibrium since  $|\dot{z}_i/\dot{y}_i| = 1$  if  $y_i = z_i$  (phase ② in Fig. 2B). While on the separatrix, any perturbation (cellular noise) in the dynamics of  $y_i$  or  $z_i$  in (3) would push the trajectory off the separatrix into either of the two basins of attraction, eventually converging to the corresponding stable equilibria in Fig. 1A (phase ③ in Fig. 2B). Importantly, perturbations in the  $j^{\text{th}}$  subsystem do not push trajectories off the separatrix in the  $(y_i, z_i)$ -plane (as  $|\dot{z}_i/\dot{y}_i| = 1$  on this separatrix, irrespective of  $y_j$  or  $z_j$  for  $j \neq i$ ). Therefore, toggles are switched independently from each other (illustrated in the simulation results of Fig. 2C), thus collectively realizing an  $N$ -bit cellular random number generator.

This  $N$ -bit binary random variable can also be converted to a scalar random number (Fig. 2A). With production rate constants  $q_i$  for the  $N$  bits we have  $\dot{v} = \sum_{i=1}^N q_i/(1+z_i^2) - v$ , thus  $v = \sum_{i=1}^N q_i/(1+z_i^2)$  at the steady state. By choosing  $q_i = 2^{i-1}q_1$ , we can convert the binary random variable  $z_1, z_2, \dots, z_N$  into the scalar  $v$  (inverted due to repression). However, this conversion is “leaky” as  $1/(1+z_i^2)$  is not precisely 0 or 1 at the non-specular equilibria, see (11). For reliable conversion, leakiness from the largest  $N-1$  bits must not cause a contribution greater than half of the contribution of the smallest bit, which is ensured if

$$\sum_{i=2}^N \frac{q_i}{1+z_i^2} < \frac{1}{2} \frac{q_1}{1+z_1^2},$$

where  $z_1 = \frac{\alpha}{2\beta} (1 - \sqrt{1 - 4\beta^2/\alpha^2})$ ,  $z_2 = \dots = z_N = 1/z_1$  with  $\beta$  from Thm. 3. The above condition can be written as

$$N \leq \log_2 \left[ 4 + \left( \frac{\alpha}{2\beta} \right)^2 \left( 1 - \sqrt{1 - \frac{4\beta^2}{\alpha^2}} \right)^2 \right] - 1. \quad (16)$$

Therefore, for a 2-bit, 5-bit, and 10-bit scalar random generator we need  $\beta \leq 0.4\alpha$ ,  $\beta \leq 0.127\alpha$ , and  $\beta \leq 0.022\alpha$ , respectively (Fig. 2D). Decreasing  $\beta/\alpha$  can be realized in multiple ways, for instance, by decreasing the dissociation constant of the repressors to the matching promoters (for details, see section S1 in the Supplementary Material).

## V. DISCUSSION

The design of large-scale complex systems relies on the predictable collective behavior of modules. As a result,

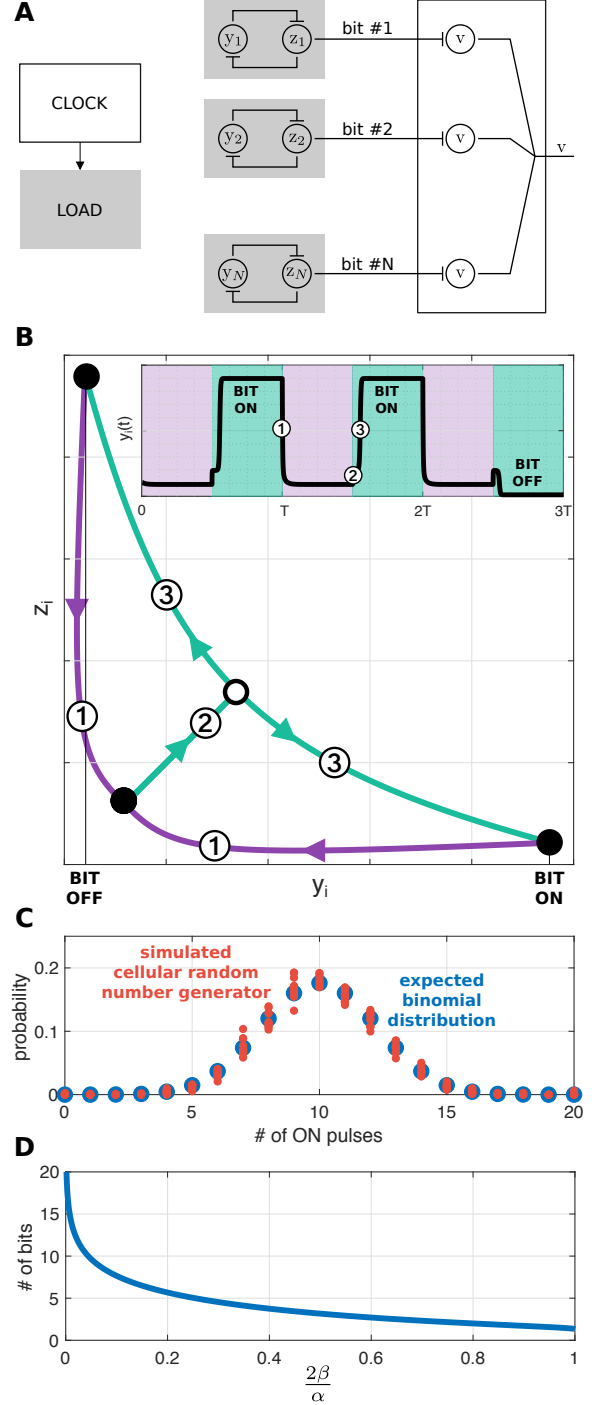


Fig. 2. Competition for shared cellular resources can be leveraged to implement an  $N$ -bit cellular random number generator. (A) The modules shaded in gray compete for shared resources. Other modules use orthogonal resources [16]. (B) By turning on (purple) and off (green) the load module, the network in (3) alternates between monostable and multistable modes. (C) The outputs of the toggle switches are independent Bernoulli random variables with success probability  $p = 0.5$ . Therefore, the output sequence on each channel is a binomial random variable, confirmed by simulation results ( $\alpha = 50$ ,  $\beta_i = i/10$ ,  $N = 10$ ,  $\beta_L^{\text{MULTI}} = 0$ ,  $\beta_L^{\text{MONO}} = 25$ ,  $T = 25$ , 1000 sequences (for details, see Tab. S1 in the Supplementary Material based on [12], [21], [22], [23], [24], [25]). (D) Increasing the ratio  $\beta/\alpha$  decreases the number of bits that can be reliably converted to the scalar random variable  $v$ , as shown in (A).

resource competition and the resulting coupling phenomenon play a central role in the progress of synthetic biology.

Therefore, in this paper we focused on the collective behavior of a network of toggle switches in the presence of scarce resources, intertwining the behavior of otherwise disconnected modules. To account for this effect, we considered a model that accurately describes and predicts experimental data obtained both *in vitro* and *in vivo* [12], [13].

Resource sequestration plays a role similar to repression as resources used by one gene become unavailable for others. Thus, it would be tempting to think that it facilitates the bistability of the toggle switch, a module based on the strong mutual repression of two genes. Surprisingly, the opposite is true: a single toggle switch is bistable only if resource competition is sufficiently low (Thm. 2), and this result naturally extends to the case when multiple toggle switches compete for the same pool of resources (Thm. 3). This can be understood by realizing that in addition to repressing the expression of other genes, competition for shared resources introduces self-repression (negative feedback) as well.

Our results also reveal that the collective behavior of multiple modules (in this case, a network of toggle switches) can be shaped without any direct regulatory linkages, solely relying on indirect effects due to resource competition. In particular, we demonstrated that (1) bistable toggle switches can become collectively monostable, and (2) the network of toggles can be switched between monostable and multistable modes by turning on/off a load module.

This idea emphasizes one of the key novelties of this paper. While the effects of resource competition are often considered detrimental [26], here we highlight how they can be leveraged instead to engage with complex systems. Rather than minimizing its effects, we can embrace the scarcity of resources and take advantage of this phenomenon ubiquitous in living systems, for instance, to implement an  $N$ -bit cellular random generator. In addition to being fundamental in both cryptography and cybersecurity, thus potentially having a central role in biosecurity, random number generators could also be employed to improve circuit performance. For instance, (biased) random walks based on the module presented in this paper could be used to implement hill climbing optimization methods without the knowledge of the gradient.

Our current ongoing work is targeted at characterizing the stability profile in the gap between (10) and (12), as well as extending the results to the case when  $\alpha_y \neq \alpha_z$ . Additionally, complementing the results presented here, future research directions involve exploring how the limited availability of shared resources can be leveraged (1) to synchronize the collective behavior of multiple modules and (2) to facilitate/inhibit the emergence of spatiotemporal patterns.

## REFERENCES

- [1] J. A. J. Arpino, E. J. Hancock, J. Anderson, M. Barahona, G.-B. V. Stan, A. Papachristodoulou, and K. Polizzi, "Tuning the dials of Synthetic Biology," *Microbiol*, vol. 159, no. 7, pp. 1236–1253, 2013.
- [2] M. J. Smanski, S. Bhatia, D. Zhao, Y. Park, L. B. A. Woodruff, G. Giannoukos, D. Ciulla, M. Busby, J. Calderon, R. Nicol, D. B. Gordon, D. Densmore, and C. A. Voigt, "Functional optimization of gene clusters by combinatorial design and assembly." *Nature Biotechnology*, vol. 32, no. 12, pp. 1241–1249, 2014.
- [3] J. T. MacDonald, C. Barnes, R. I. Kitney, P. S. Freemont, and G.-B. V. Stan, "Computational design approaches and tools for synthetic biology," *Integrative Biology*, vol. 3, no. 2, pp. 97–108, 2011.
- [4] N. Crook and H. S. Alper, "Model-based design of synthetic, biological systems," *Chem Eng Sci*, vol. 103, pp. 2–11, 2013.
- [5] S. Cardinale and A. P. Arkin, "Contextualizing context for synthetic biology—identifying causes of failure of synthetic biological systems." *Biotechnology Journal*, vol. 7, no. 7, pp. 856–866, 2012.
- [6] A. Y. Weiße, D. A. Oyarzún, V. Danos, and P. S. Swain, "Mechanistic links between cellular trade-offs, gene expression, and growth," *PNAS*, vol. 112, no. 9, pp. E1038–E1047, 2015.
- [7] O. Borkowski, F. Ceroni, G. Stan, and T. Ellis, "Overloaded and stressed: whole-cell considerations for bacterial synthetic biology," *Current Opinion in Microbiology*, vol. 33, pp. 123–130, 2016.
- [8] V. H. Nagaraj, J. M. Greene, A. M. Sengupta, and E. D. Sontag, "Translation inhibition and resource balance in the TX-TL cell-free gene expression system," *Synth Biol*, vol. 2, no. 1, pp. 1–7, 2017.
- [9] S. J. Moore, J. T. MacDonald, S. Wienecke, A. Ishwarbhai, A. Tsipa, R. Aw, N. Kyllilis, D. J. Bell, D. W. McClymont, K. Jensen, K. M. Polizzi, R. Biedendieck, and P. S. Freemont, "Rapid acquisition and model-based analysis of cell-free transcription–translation reactions from nonmodel bacteria," *PNAS*, 2018.
- [10] D. Siegal-Gaskins, Z. A. Tuza, J. Kim, V. Noireaux, and R. M. Murray, "Gene Circuit Performance Characterization and Resource Usage in a Cell-Free Breadboard," *ACS Synth Biol*, vol. 3, pp. 416–425, 2014.
- [11] F. Ceroni, R. Algar, G.-B. Stan, and T. Ellis, "Quantifying cellular capacity identifies gene expression designs with reduced burden." *Nature Methods*, vol. 12, no. 5, pp. 415–418, 2015.
- [12] A. Gyorgy, J. I. Jiménez, J. Yazbek, H.-H. Huang, H. Chung, R. Weiss, and D. Del Vecchio, "Isocost Lines Describe the Cellular Economy of Genetic Circuits," *Biophys J*, vol. 109, no. 3, pp. 639–646, 2015.
- [13] A. Gyorgy and R. M. Murray, "Quantifying resource competition and its effects in the TX-TL system," in *55th IEEE Conference on Decision and Control (CDC)*. IEEE, 2016, pp. 3363–3368.
- [14] O. Purcell, M. di Bernardo, C. S. Grierson, and N. J. Savery, "A multi-functional synthetic gene network: A frequency multiplier, oscillator and switch," *PLOS ONE*, vol. 6, no. 2, pp. 1–12, 2011.
- [15] C. Cuba Samaniego and E. Franco, "A robust molecular network motif for period-doubling devices," *ACS Synthetic Biology*, vol. 7, no. 1, pp. 75–85, 2018, PMID: 29227103.
- [16] A. P. S. Darlington, J. Kim, J. I. Jimenez, and D. G. Bates, "Dynamic allocation of orthogonal ribosomes facilitates uncoupling of co-expressed genes," *Nat Comm*, vol. 9, no. 1, p. 695, 2018.
- [17] T. S. Gardner, C. R. Cantor, and J. J. Collins, "Construction of a genetic toggle switch in *Escherichia coli*," *Nature*, vol. 403, no. 6767, pp. 339–342, 2000.
- [18] D. Angeli and E. D. Sontag, "Monotone control systems," *IEEE Trans Automat Contr*, vol. 48, no. 10, pp. 1684–1698, Oct 2003.
- [19] D. Angeli and E. Sontag, "Interconnections of monotone systems with steady-state characteristics," in *Optimal Control, Stabilization and Nonsmooth Analysis*. Springer Berlin, 2004, pp. 135–154.
- [20] A. Gyorgy and M. Arcak, "Pattern formation over multigraphs," *IEEE Trans Netw Sci Eng*, vol. 5, no. 1, pp. 55–64, 2018.
- [21] S. Klump and T. Hwa, "Growth-rate-dependent partitioning of rna polymerases in bacteria," *Proceedings of the National Academy of Sciences*, vol. 105, no. 51, pp. 20 245–20 250, 2008.
- [22] H. Bremer and P. P. Dennis, "Modulation of Chemical Composition and Other Parameters of the Cell at Different Exponential Growth Rates." *EcoSal Plus*, vol. 3, no. 1, Sept. 2008.
- [23] A. Kamionka, J. Bogdanska-Urbaniak, O. Scholz, and W. Hillen, "Two mutations in the tetracycline repressor change the inducer anhydrotetracycline to a corepressor." *Nucleic Acids Research*, vol. 32, no. 2, pp. 842–847, 2004.
- [24] J. T. Kittleson, S. Cheung, and J. C. Anderson, "Rapid optimization of gene dosage in *E. coli* using DIAL strains." *Journal of Biological Engineering*, vol. 5, no. 1, p. 10, July 2011.
- [25] J. A. Bernstein, A. B. Khodursky, P.-H. Lin, S. Lin-Chao, and S. N. Cohen, "Global analysis of mRNA decay and abundance in *Escherichia coli* at single-gene resolution using two-color fluorescent DNA microarrays." *PNAS*, vol. 99, no. 15, pp. 9697–9702, July 2002.
- [26] Y. Qian, H.-H. Huang, J. I. Jiménez, and D. Del Vecchio, "Resource Competition Shapes the Response of Genetic Circuits," *ACS Synthetic Biology*, vol. 6, no. 7, pp. 1263–1272, 2017.